

Anomalous transport properties of $R\text{Fe}_4\text{P}_{12}$ ($R = \text{La, Ce, Pr, and Nd}$)

H. Sato, Y. Abe, H. Okada, T. D. Matsuda, K. Abe, H. Sugawara, and Y. Aoki

Department of Physics, Tokyo Metropolitan University, Tokyo 192-0397, Japan

(Received 29 February 2000)

We have investigated the resistivity (ρ), thermoelectric power (TEP), and Hall coefficient (R_H) on high-quality single crystals of $R\text{Fe}_4\text{P}_{12}$. TEP in $\text{CeFe}_4\text{P}_{12}$ is extremely large (~ 0.5 mV/K at 290 K) with a peak of ~ 0.75 mV/K at around 65 K. The Hall mobility also shows a peak at ~ 65 K, suggesting carriers with heavy masses developed at lower temperatures related to the f -hybridized band. Both Pr and Nd systems exhibit an apparent increase of ρ with decreasing temperature far above their magnetic transition temperatures. In the same temperature ranges, TEP exhibits unusually large absolute values of -50 $\mu\text{V/K}$ for $\text{PrFe}_4\text{P}_{12}$ and -15 $\mu\text{V/K}$ for $\text{NdFe}_4\text{P}_{12}$, respectively. For $\text{PrFe}_4\text{P}_{12}$, such anomalous transport properties suggest an unusual ground state, possibly related to the quadrupolar Kondo effect.

I. INTRODUCTION

Recently, the rare-earth (RE) compounds RT_4P_{12} (T : Fe, Co, Ru, Os; P : P, As, Sb) with filled skutterudite structure¹⁻³ have attracted much attention, partly because of a potential practical application as thermoelectric materials.^{4,5} Also from the viewpoint of basic physics, a number of novel phenomena, such as a metal-insulator transition and intermediate valence, have been reported.⁶⁻⁸ Torikachvili *et al.*² have reported a systematic study of $R\text{Fe}_4\text{P}_{12}$ where they found a variety of interesting properties depending on RE atoms—i.e., superconducting $\text{LaFe}_4\text{P}_{12}$ below 4.2 K, insulating $\text{CeFe}_4\text{P}_{12}$, antiferromagnetic $\text{PrFe}_4\text{P}_{12}$ below 6.4 K, and ferromagnetic $\text{NdFe}_4\text{P}_{12}$ below 1.9 K. A uranium analog $\text{UFe}_4\text{P}_{12}$ was also reported to be insulating.⁹ For a better understanding of these novel phenomena, high-quality single crystals are essential. We have recently succeeded in growing high-quality $R\text{Fe}_4\text{P}_{12}$ single crystals that realized the first de Haas–van Alphen (dHvA) experiment.¹⁰ In this paper, we report a first experimental study (except for our preliminary report in the SCES'98 proceedings¹¹) on the thermoelectric power and Hall effect of $R\text{Fe}_4\text{P}_{12}$ single crystals along with the anomalous behaviors in the electrical resistivity.

II. EXPERIMENT

Single crystals were grown by the tin-flux method,¹ using 99.99% Fe, La, Ce, and Pr, 99.9% Nd, 99.9999% P, and 99.999% Sn. The samples for transport measurements are basically the same as were used for dHvA measurements,¹⁰ and both measurements were made on exactly the same samples for some compounds. Their Dingle temperatures were estimated to be 0.3–0.6 K, which ensures samples of high quality. The high quality is also reflected in the large residual resistance ratio (RRR) of 1300 and 1000 for La and Nd samples, respectively. The small RRR of ~ 13 for $\text{PrFe}_4\text{P}_{12}$ at zero field does not indicate a low sample quality, since the Fermi surface (FS) changes across T_N . The intrinsic RRR of $\text{PrFe}_4\text{P}_{12}$ was estimated to be ~ 1000 from the resistivity at 0.3 K in high fields above the metamagnetic transition. We found a meaningful correlation between the dHvA amplitude and the RRR; i.e., the dHvA oscillations

could be detected only in large RRR samples. The electrical resistivity and Hall resistivity were measured by the ordinary dc four-probe method. The temperature was monitored by calibrated two RuO_2 and one platinum resistance thermometers depending on temperature ranges between 0.5 and 295 K. The calibration was made against a thin-film resistance temperature sensor (Cernox resistor, Lake Shore) calibrated against the International Temperature scale of 1990 (ITS-90). In a supplemental cryostat used only above 1.5 K, a Au–0.07% Fe vs Chromel thermocouple was used as a temperature monitor. The thermoelectric power was measured by the differential method using Au–0.07% Fe vs Chromel thermocouples. The thermocouples were calibrated after every cooling down at the boiling point of ^4He in ambient pressure. The accuracy of the temperature measurement is less than 0.1 K at low temperatures, while it is a few K near room temperature (RT). The voltage measurements were made by Keithley 182 nanovoltmeters. The magnetic measurements were made by a Quantum Design superconducting quantum interference device (SQUID) magnetometer up to 5.5 T.

III. RESULTS AND DISCUSSION

A. Electrical resistivity

The temperature dependence of the electrical resistivity $\rho(T)$ for $\text{LaFe}_4\text{P}_{12}$ (not shown) almost agrees with the result in Ref. 2 except the orders of magnitude larger RRR in the present work. The superconducting transition temperature (T_S) estimated from the midpoint of the resistive transition is 4.6 K with a transition width of $\Delta T \sim 0.6$ K. The higher T_S in the $\rho(T)$ measurement is not attributable to the reported enhancement of T_S with pressure in $\text{LaFe}_4\text{P}_{12}$,¹² since T_S estimated from a SQUID measurement under almost the same sample condition is 4.17 K, in agreement with the previous report.² The transition in $\rho(T)$ may not be a bulk property, but is plausibly the surface superconductivity as is occasionally observed in rare-earth superconductors. In fact, $\rho(T)$ for $\text{LaFe}_4\text{P}_{12}$ in Ref. 2 also shows a tendency to decrease at around 7 K. Below 25 K, ρ is well described by $\rho(T) = \rho_0 + A_0 T^2$, with $A_0 = (1.0 \pm 0.1) \times 10^{-3}$ $\mu\Omega \text{ cm K}^{-2}$. The

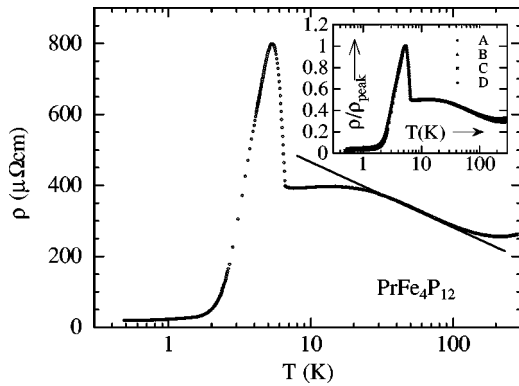


FIG. 1. Temperature dependence of the electrical resistivity for $\text{PrFe}_4\text{P}_{12}$. The inset shows the $\rho(T)$'s on four different samples normalized at the peak, where the difference is only barely discernible.

large A_0 compared to the ordinary metals reflects a large contribution from the $3d$ band of Fe to the electronic density of states at the Fermi level, as was already indicated in the large specific heat coefficient.¹³

Figure 1 shows the temperature dependence of the resistivity for $\text{PrFe}_4\text{P}_{12}$. The most remarkable difference in $\rho(T)$ for $\text{PrFe}_4\text{P}_{12}$ between the present work and Ref. 2 is the sign of $d\rho/dT$ above the Néel temperature (T_N). In Fig. 1, $\rho(T)$ increases almost logarithmically with decreasing temperature between 100 and 30 K, in contrast with the monotonic decrease from RT down to T_N in Ref. 2. The absolute value of $\rho(T)$ is slightly sample dependent in the present work due to the irregular shapes of the samples. However, $\rho(T)$'s normalized at the peak for four samples from different batches lie almost on a single curve as shown in the inset of Fig. 1. The negative $d\rho/dT$ is reminiscent of the Kondo effect that has been frequently observed in Ce and U compounds. For Pr compounds, PrSn_3 (Ref. 14) and PrInAg_2 (Ref. 15) are the quite rare examples exhibiting the Kondo behaviors. A notable feature of $\text{PrFe}_4\text{P}_{12}$ compared to these two compounds is a large magnitude of the logarithmic increase in $\rho(T)$. A large C_e/T value (>1 J/molK²) reported at low temperatures in the high-field paramagnetic state,¹⁶ indicating the existence of mass-enhanced electrons, is another sign of the Kondo effect in $\text{PrFe}_4\text{P}_{12}$. If the logarithmic increase in $\rho(T)$ is ascribed to the Kondo scattering, the Kondo temperature T_K should be ~ 100 K. The T_K value is in conflict with the Weiss temperature (θ_p) of a few K, which provides a measure of T_K for heavy fermion compounds, though Kondo scattering associated with higher crystal field levels could not be ruled out as an origin of such an enhancement of T_K in $\rho(T)$.¹⁷ The origin of the logarithmic increase in ρ is an attractive subject for further investigations.

With decreasing temperature, ρ shows a sharp upturn at 6.7 K followed by a peak around 5.4 K. The general features agree with the result in Ref. 2, although the ratio $RR = \rho(7.5 \text{ K})/\rho(0.5 \text{ K}) = 12\text{--}20$ in the present experiment shows a sharp contrast with $RR < 1$ in Ref. 2. A notable feature in Fig. 1 is an abrupt change in slope of $\rho(T)$ curves at ~ 2 K, which was already found on one of the samples in Ref. 2. A sudden increase in $\rho(T)$ above 2 K suggests some gap structure in the scattering probability. Tentatively assuming a resistivity component with the form ρ_G

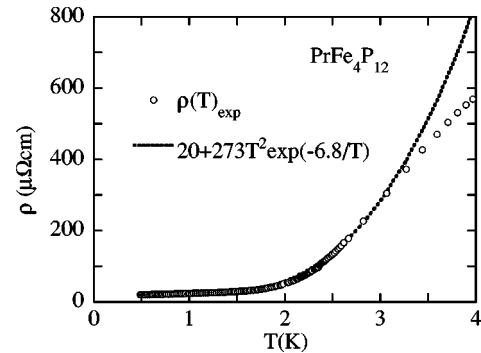


FIG. 2. Comparison of the experimental $\rho(T)$ for $\text{PrFe}_4\text{P}_{12}$ with the temperature dependence expected for the scattering with a gap structure.

$=A_1 T^2 \exp(-\Delta/k_B T)$,¹⁸ $\rho(T)$ below 3.2 K is well reproduced by using $\Delta/k_B = 6.8$ K as given in Fig. 2. This fact suggests that the scattering probability of conduction electrons reflects some gap structure, probably in the magnon dispersion relation, although the agreement of $\Delta/k_B = 6.8$ K with T_N may be accidental. It should be noted that a bend was observed near 2 K also in the temperature dependence of the specific heat coefficient.¹⁶

$\rho(T)$ for $\text{NdFe}_4\text{P}_{12}$ is in agreement with that in Ref. 2 except for the low residual resistivity ($< 1/20$) in the present experiment. Figure 3 shows the low-temperature part of $\rho(T)$ for $\text{NdFe}_4\text{P}_{12}$ where $d\rho/dT$ is negative between ~ 4 and 30 K. The negative $d\rho/dT$ developing below $\sim 10 \times T_C$ is quite unusual for ferromagnetic materials. The minimum should be intrinsic, since it has been reproducibly observed in samples with large RRR values. Below a sharp drop at $T_C \sim 2$ K, the exponent N in $\rho(T) = \rho_0 + A_0 T^N$ is close to 4 as shown in the inset. The exponent, twice as large as $N=2$ expected for simple magnon scattering, is well correlated with the T^3 dependence of the specific heat reported in Ref. 2 (in contrast with the $T^{3/2}$ dependence expected for simple ferromagnets). Such large exponents for both the resistivity and specific heat could be consistently understood,¹⁹ if the magnon dispersion relation is $\hbar\omega \propto q$ rather than $\hbar\omega \propto q^2$.

Figure 4 shows $\rho(T)$ in $\text{CeFe}_4\text{P}_{12}$ for four different samples. The resistivity change between RT and the lowest temperature in the present experiment is about five orders of magnitude smaller than that in Ref. 2. It should be noted

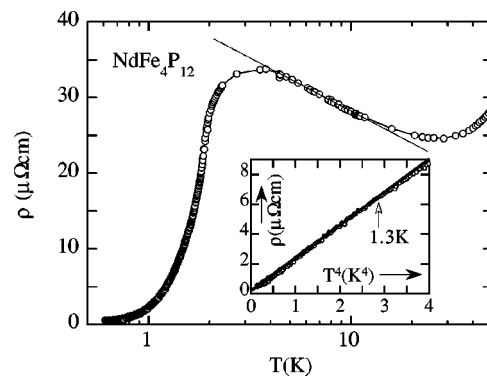


FIG. 3. Temperature dependence of resistivity for $\text{NdFe}_4\text{P}_{12}$. The inset shows the ρ vs T^4 plot.

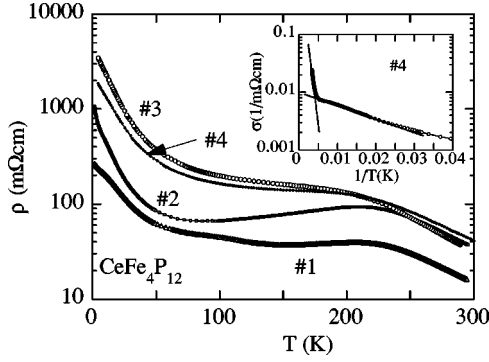


FIG. 4. Temperature dependence of resistivity for four different $\text{CeFe}_4\text{P}_{12}$ samples. The inset shows the $\log(\sigma)$ vs T^{-1} plot for No. 4.

again that dHvA signals with large effective masses have been detected in La-, Pr-, and Nd- Fe_4P_{12} (Refs. 10 and 20) grown by the same procedure as described above, ensuring the quality of the bulk part of the samples. We thus infer that the effect of impurity doping on the bulk part of the samples might be less in the present work. Taking into account these facts, some shortening effect by small size grains of Sn inevitably embedded in the sample is the most probable origin for such a difference in $\rho(T)$ between the two works. We have tried to reduce the embedded Sn grains by following two approaches: (1) repeatedly slicing and etching a sample in acid to dissolve Sn and (2) selecting samples from different crystals from different batches. From the Meissner diamagnetic contribution to the low-field magnetic susceptibility, we have found the amount of Sn to vary from ~ 1 to less than 0.01 vol%. However, despite the large variation in the Sn content, only a minor change in $\Delta\rho/\rho_{280\text{ K}} = (\rho_{1.5\text{ K}} - \rho_{280\text{ K}})/\rho_{280\text{ K}}$ was observed. Note that a large sample-to-sample variation in the conducting behavior in $\text{CeFe}_4\text{P}_{12}$ was already reported in Refs. 3 and 21, although the $\rho(T)$ curve was shown only for a single sample. It should be also noted that the resistivity at RT in the present work is slightly larger than that estimated in Ref. 21.

The temperature dependence of ρ in Fig. 4 indicates the existence of three characteristic temperature ranges, i.e., $T > 230\text{ K}$, $230\text{ K} > T > 50\text{ K}$, and $T < 50\text{ K}$. The energy gap of 1250 K estimated from the $\rho(T)$ data above 250 K is almost sample independent. The value is close to the reported value of 1500 K in Ref. 3 which was estimated in the temperature range $85\text{ K} < T < 140\text{ K}$. These values are about 1/3 of the gap ($=0.34\text{ eV}$) estimated by the band structure calculation within the local-density approximation.²² Taking into account the fact that a recent optical experiment also gives a smaller gap of 0.15 eV,²¹ the disagreement may be ascribed to a local-density approximation that tends to overestimate the band gaps.²² $\rho(T)$ depends only slightly on temperature from 230 K to $\sim 50\text{ K}$ below which it shows a sharp upturn. The upturn below 50 K, which is hardly explainable if the shortening effect of metallic Sn grains dominates the conduction, is probably an intrinsic behavior of $\rho(T)$. At this stage, we cannot give any conclusive remark on the origin of the difference in $\rho(T)$ behaviors in the two works. However, it might be worthwhile to report the first Hall effect and thermoelectric power experiments on $\text{CeFe}_4\text{P}_{12}$, since the main characteristics are reproducible.

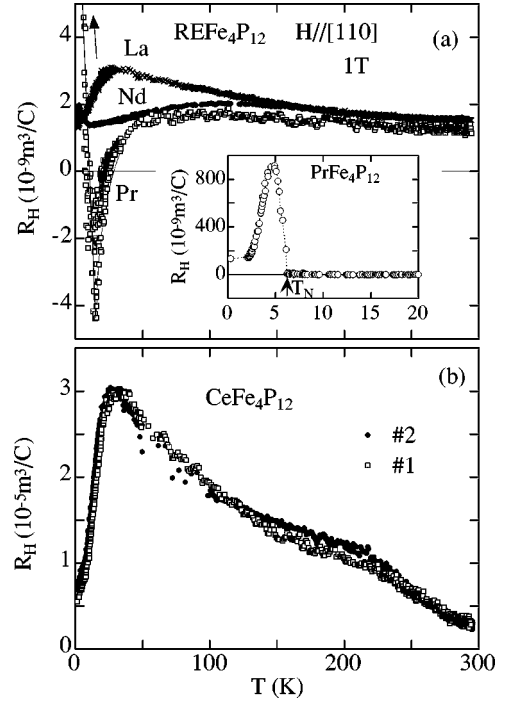


FIG. 5. Temperature dependence of the Hall coefficient (a) for La-, Pr-, and Nd- Fe_4P_{12} and (b) for $\text{CeFe}_4\text{P}_{12}$.

B. Hall effect

Figure 5 shows the temperature dependence of the Hall coefficient R_H for (a) La-, Pr-, and Nd- Fe_4P_{12} and (b) $\text{CeFe}_4\text{P}_{12}$. At RT, R_H is $\sim 1.5 \times 10^{-9}\text{ m}^3/\text{C}$ for both La- and Nd- Fe_4P_{12} , and $\sim 1.3 \times 10^{-9}\text{ m}^3/\text{C}$ for Pr- Fe_4P_{12} . The Hall coefficient in magnetic systems is usually expressed as a combination of the normal Hall coefficient R_{H0} resulting from the Lorentz motion of conduction electrons and the extraordinary one R_{ex} caused by magnetic scattering of conduction electrons: $R_H = R_{H0} + R_{ex}$.²³⁻²⁵ The positive R_H at RT, where R_{H0} dominates, is consistent with the band structure calculation for La Fe_4P_{12} predicting two-hole-like Fermi sheets.²⁶ The weak temperature dependence of R_H for La Fe_4P_{12} , including a peak at 25 K, can be understood as due to the temperature dependence of the anisotropy in the relaxation time $\tau(\mathbf{k})$.²⁷ As shown in the inset of Fig. 5(a), the change in R_H below T_N for Pr Fe_4P_{12} is more than two orders of magnitude larger than that above T_N , which also indicates a FS reconstruction associated with the antiferromagnetic superzone gap formation. $R_H(T)$ becomes almost temperature independent below 2 K, which also suggests some gap structure described above in correlation with the anomalies in $\rho(T)$ and the specific heat.¹⁶

At temperatures higher than Kondo temperature,^{24,25} R_{ex} in the dense Kondo compounds has been well described by the skew scattering mechanism as $R_{ex} = \gamma \chi_{red} \times \rho_m$, using the reduced magnetic susceptibility χ_{red} , the magnetic part of the resistivity ρ_m , and a parameter γ depending on the phase shift associated with the Kondo scattering. To test the model, R_H is compared with $M \times \rho$ calculated from the magnetization at 0.1 T and zero-field resistivity for Pr Fe_4P_{12} as a function of temperature in Fig. 6(a). Here $R_H(T)$ is qualitatively reproduced by the $M \times \rho$ curves above T_N . In contrast, the experimental curve for Nd Fe_4P_{12} is hardly reproduced

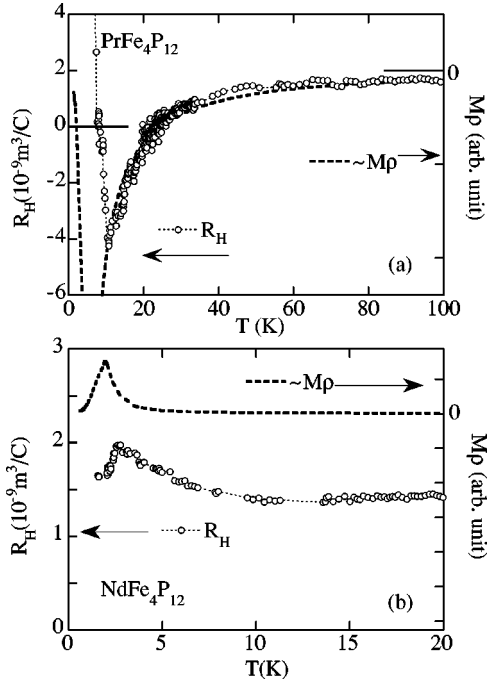


FIG. 6. Comparison of experimental R_H with the skew scattering contribution $\sim M\rho$. (a) for $\text{PrFe}_4\text{P}_{12}$ and (b) for $\text{NdFe}_4\text{P}_{12}$.

over the wide temperature range, even if the temperature dependence of R_{H0} is taken into account. This fact suggests that the skew scattering contribution is small at high temperatures. Thus, the comparison between R_H and $M \times \rho$ is shown in Fig. 6(b) only near T_C , where the extraordinary Hall resistivity $R_S M$ is expected to become larger.²³ The positive peak is well reproduced as a combined effect of growing M and decreasing ρ below T_C , though the peak for R_H is broader and shifted to higher temperatures. The disagreement could be partly ascribed to the higher applied field of 1 T in the R_H measurement.

For $\text{CeFe}_4\text{P}_{12}$, despite the clear difference in the $\rho(T)$ curves, $R_H(T)$'s for the two different samples (Nos. 1 and 2) are basically same including the absolute values, suggesting the overall feature of R_H to be a bulk property. Corresponding to the hump in $\rho(T)$, a change in the slope of $R_H(T)$ exists around 220 K. A notable feature in Fig. 5(b) is a sharp drop of R_H below a peak at ~ 25 K in correlation with the low-temperature upturn in $\rho(T)$. Below RT, the sign is always positive, suggesting higher mobility carriers in the top valence band. Of course, the existence of acceptor-type impurities could not be ruled out at this stage. Assuming the single-carrier model, the concentration of carriers is estimated to be 1×10^{-3} holes/f.u. at RT, 1×10^{-4} holes/f.u. at 25 K (peak in R_H), and 4×10^{-4} holes/f.u. at 2 K.

The combination of decreasing R_H and increasing $\rho(T)$ with decreasing T leads to a decrease of Hall mobility below 25 K based on the single-carrier model as shown in Fig. 7. The Hall mobility at RT is about an order of magnitude smaller than that in Si.²⁷ The decrease in Hall mobility above ~ 150 K with increasing T follows a $T^{-3/2}$ dependence, suggesting the dominant acoustic phonon scattering as expected for ordinary semiconductors.²⁸ Note the apparent peak in the Hall mobility observed around 65 K.

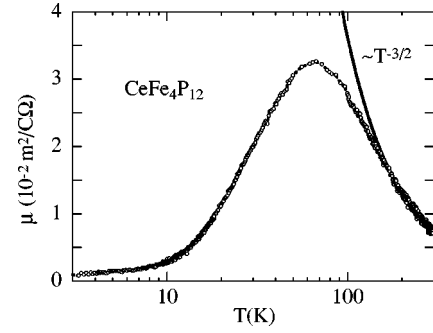


FIG. 7. Temperature dependence of the Hall mobility in $\text{CeFe}_4\text{P}_{12}$ calculated by using $\rho(T)$ and $R_H(T)$ data.

C. Thermoelectric power

Figure 8(a) shows the temperature dependence of TEP for La, Pr, and Nd compounds. TEP for $\text{LaFe}_4\text{P}_{12}$ decreases with decreasing T from $\approx 9 \mu\text{V/K}$ at 290 K, and changes its sign below 18 K after showing a minimum near 200 K and a maximum near 100 K. The relatively large absolute value at RT compared to simple metals is ascribable to the large contribution from the $3d$ band of Fe at the Fermi surface.^{26,29} A delicate combination of the diffusion and the phonon drag contributions might lead to such a complex T dependence.

TEP for $\text{NdFe}_4\text{P}_{12}$ is almost indistinguishable with that of $\text{LaFe}_4\text{P}_{12}$ above 220 K, suggesting a localized nature of $4f$ electrons in this system. At lower temperatures, TEP deviates from that for $\text{LaFe}_4\text{P}_{12}$ downward and changes its sign at around 85 K. At the lowest temperature, it approaches zero after showing a minimum of $\sim 15 \mu\text{V/K}$ which is quite large as a localized f -electron material. The coincidence of the minimum temperature (~ 30 K) with that for the $\rho(T)$ minimum suggests that these minima originate from the same conduction-electron scattering with a characteristic energy scale of ~ 30 K.

TEP for $\text{PrFe}_4\text{P}_{12}$ shows largely different behaviors. Even at 290 K, the magnitude is about twice as large as that in

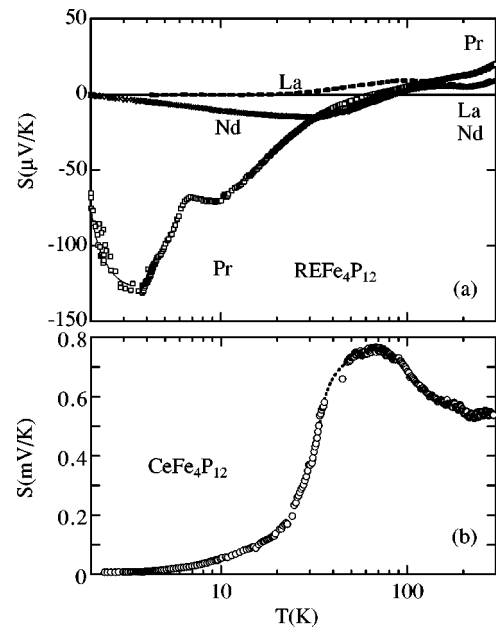


FIG. 8. Temperature dependence of thermoelectric power (a) for La-, Pr-, and Nd- Fe_4P_{12} and (b) for $\text{CeFe}_4\text{P}_{12}$.

LaFe₄P₁₂, and decreases with decreasing T . Below a sign change near 70 K, it drastically decreases with T , showing a bend near T_N . After exhibiting a large minimum near 3 K, it approaches to 0 $\mu\text{V/K}$ at the lowest temperature. The sharp drop below T_N could be ascribed to the FS reconstruction. However, the large magnitude ($\sim 50 \mu\text{V/K}$) above T_N is quite unusual.

The diffusion thermoelectric power is represented by an energy derivative of conductivity $\sigma(\varepsilon)$ as³⁰

$$S = -(\pi^2 k_B^2 T / 3e\sigma) \{d\sigma(\varepsilon)/d\varepsilon\}_{\varepsilon_F}.$$

The origins of the energy dependence of $\sigma(\varepsilon)$ could be further classified into two factors; carrier numbers and scattering probability. In the high-mobility semiconductors where the former factor is huge, a large value of TEP could be expected at low temperatures. It is not applicable to PrFe₄P₁₂, since we already know the existence of rather large FS's in PrFe₄P₁₂ from dHvA experiments.²⁰ Even in the transition metals and alloys with a large electronic density of states near the Fermi energy, a large diffusion TEP has been reported only at high temperatures.³¹ In fact, this is the case for TEP in LaFe₄P₁₂. Such a large magnitude of TEP in metals with a large FS has been reported only for Kondo systems where a large energy-dependent scattering process is essential.^{31,32} If we assume 4*f* electrons to be well localized in PrFe₄P₁₂, the difference compared to the La and Nd compounds should be ascribed only to the electron scattering by the localized 4*f* electrons. Then, we can hardly expect such a large magnitude of TEP at low temperatures and a difference in TEP at RT compared to LaFe₄P₁₂. The small sample size could lead to a large error in TEP; however, we confirmed the contribution to be minor in the present case from independent measurements on different samples.

Figure 8(b) shows the T dependence of TEP for CeFe₄P₁₂, where the huge value of TEP should be noted. At around 65 K, TEP exhibits a broad peak of $\sim 0.76 \text{ mV/K}$ and sharply decreases below 50 K where $\rho(T)$ shows an apparent increase after a plateau. The temperature dependence is weak above 100 K, except a small but an apparent anomaly at

$\sim 220 \text{ K}$. The positive sign of TEP as well as R_H at high temperatures is consistent with the band structure calculation.²⁹ The top valence bands are dominated by the hybridized Fe 3*d* and P 3*p* states with a moderate dispersion, while the lowest conduction bands are dominated by the narrow spin-orbit-split Ce 4*f* bands. Namely, the effective mass for the electrons in the 4*f*-dominated bands is apparently heavier than that for the holes in the valence bands, which leads to the positive TEP and R_H in the intrinsic regime.

IV. CONCLUSIONS

All the transport properties of CeFe₄P₁₂ show unusual temperature dependence below RT: the complex temperature dependence of resistivity unexpected for a simple single-gap semiconductor, the huge thermoelectric power above $\sim 10 \text{ K}$ with a maximum value of 0.76 mV/K, the sharp decrease of both TEP, and the carrier mobility below a peak around 65 K. All these features might be related to the 4*f*-electron hybridization associated with the filled skutterudite structure as was already pointed out based on the electrical resistivity and optical measurements.

The most remarkable finding was made on PrFe₄P₁₂. All the transport properties $\rho(T)$, $R_H(T)$, and $S(T)$ indicate the strong possibility of Kondo-like scattering. The ordinary magnetic Kondo effect may not be its origin. In order to clarify the origin, further investigations such as neutron scattering and ultrasonic experiments are in progress.

The negative dp/dT above T_C in NdFe₄P₁₂ has a magnetic origin, which might be related to an unusual dispersion of the magnon spectrum inferred from the temperature dependence of the resistivity and the specific heat below T_C .

ACKNOWLEDGMENTS

The authors are grateful to thank Professor Y. Onuki, Professor H. Harima, and Professor O. Sakai for helpful discussions. This work was partly supported by a Grant-in-Aid for Scientific Research from the Ministry of Education, Science, Sports and Culture of Japan.

¹W. Jeitschko and D. Braun, Acta Crystallogr., Sect. B: Struct. Crystallogr. Cryst. Chem. **33**, 3401 (1977).

²M. S. Torikachvili, J. W. Chen, Y. Dalichaouch, R. P. Guertin, M. W. McElfresh, C. Rossel, M. B. Maple, and G. P. Meisner, Phys. Rev. B **36**, 8660 (1987), and references therein.

³G. P. Meisner, M. S. Torikachvili, K. N. Yang, M. B. Maple, and R. P. Guertin, J. Appl. Phys. **57**, 3073 (1985).

⁴B. C. Sales, D. Mandrus, and R. K. Williams, Science **272**, 1325 (1996).

⁵G. Mahan, B. Sales, and J. Sharp, Phys. Today **50** (3), 43 (1997).

⁶C. Sekine, T. Uchiumi, I. Shirovani, and T. Yagi, Phys. Rev. Lett. **79**, 3218 (1997).

⁷N. R. Dilley, E. J. Freeman, E. D. Bauer, and M. B. Maple, Phys. Rev. B **58**, 6287 (1998).

⁸N. Takeda and M. Ishikawa, Physica B **259-261**, 92 (1999).

⁹M. S. Torikachvili, C. Rossel, M. W. McElfresh, M. B. Maple, R.

P. Guertin, and G. P. Meisner, J. Magn. Magn. Mater. **54-57**, 365 (1986).

¹⁰H. Sugawara, Y. Abe, Y. Aoki, H. Sato, M. Hedo, R. Settai, and Y. Onuki, J. Magn. Magn. Mater. **177-181**, 359 (1998); H. Sugawara, Y. Abe, Y. Aoki, H. Sato, M. Hedo, R. Settai, Y. Onuki, and H. Harima, J. Phys. Soc. Jpn. **69**, 2938 (2000).

¹¹H. Sato, Y. Abe, H. Okada, T. D. Matsuda, H. Sugawara, and Y. Aoki, in Proceedings of SCES'98 [Physica B **281&282**, 306 (2000)].

¹²L. E. Delong and G. P. Meisner, Solid State Commun. **53**, 119 (1985).

¹³G. P. Meisner, G. R. Stewart, M. S. Torikachvili, and M. B. Maple, Proc. LT-17, 171 (1984).

¹⁴P. Lethuillier and P. Haen, Phys. Rev. Lett. **35**, 1391 (1975).

¹⁵A. Yatskar, W. P. Beyermann, P. Movshovich, and P. C. Canfield, Phys. Rev. Lett. **77**, 3637 (1996).

- ¹⁶T. D. Matsuda, H. Okada, H. Sugawara, Y. Aoki, H. Sato, A. V. Andreev, Y. Shiokawa, V. Sechovsky, T. Honma, E. Yamamoto, and Y. Onuki, *Physica B* **281&282**, 220 (2000).
- ¹⁷K. Yamada, K. Yoshida, and K. Hanzawa, *Prog. Theor. Phys.* **71**, 450 (1984).
- ¹⁸K. A. McEwen, in *Handbook on the Physics and Chemistry of Rare Earth*, edited by K. A. Gschneidner, Jr. and L. Eyring (North-Holland, Amsterdam, 1978), p. 411.
- ¹⁹I. Mannari, *Prog. Theor. Phys.* **22**, 335 (1959).
- ²⁰H. Sugawara, T. D. Matsuda, K. Abe, Y. Aoki, H. Sato, S. Nojiri, Y. Inada, R. Settai, and Y. Onuki (unpublished).
- ²¹S. V. Dordevic, N. R. Dilley, E. D. Bauer, D. N. Basov, M. B. Maple, and L. Degiorgi, *Phys. Rev. B* **60**, 11 321 (1999).
- ²²L. Nordström and D. J. Singh, *Phys. Rev. B* **53**, 1103 (1996).
- ²³C. M. Hurd, *The Hall Effect in Metals and Alloys* (Plenum Press, New York, 1972).
- ²⁴P. Coleman, P. W. Anderson, and T. V. Ramakrishnan, *Phys. Rev. Lett.* **55**, 414 (1985).
- ²⁵A. Fert and P. M. Levy, *Phys. Rev. B* **36**, 1907 (1987).
- ²⁶H. Harima, *J. Magn. Magn. Mater.* **177-181**, 321 (1998).
- ²⁷R. G. Chambers, *Electrons in Metals and Semiconductors* (Chapman and Hall, London, 1990).
- ²⁸P. P. Debye and E. M. Conwell, *Phys. Rev. B* **93**, 693 (1954).
- ²⁹M. Fornari and D. Singh, *Phys. Rev. B* **59**, 9722 (1999).
- ³⁰J. S. Dugdale, *The Electrical Properties of Metals and Alloys* (Edward Arnold, London, 1977).
- ³¹J. M. Fournier and E. Gratz, in *Handbook on the Physics and Chemistry of Rare Earths*, edited by K.A. Gschneidner, Jr., L. Eyring, G. H. Lander, and G. R. Choppin (Elsevier Science, New York, 1993), Vol. 17, Chap. 115.
- ³²D. Jaccard and J. Sierro, in *Valence Instabilities*, edited by P. Wachter and H. Boppart (North-Holland, Amsterdam, 1982), p. 409.